01 Jan 1986

CLOSED-LOOP DYNAMIC RESPONSE OF A STATIC SCHERBIUS DRIVE.

Aaron J. Miles
Missouri University of Science and Technology

B. Lequesne

Recommended Citation

A. J. Miles and B. Lequesne, "CLOSED-LOOP DYNAMIC RESPONSE OF A STATIC SCHERBIUS DRIVE.," *PESC Record - IEEE Annual Power Electronics Specialists Conference*, pp. 510 - 515, Institute of Electrical and Electronics Engineers, Jan 1986.
The definitive version is available at https://doi.org/10.1109/pesc.1986.7415601

CLOSED-LOOP DYNAMIC RESPONSE OF A STATIC SCHERBIUS DRIVE

A. R. Miles
University of Missouri-Rolla
Rolla, Missouri 65401

B. Lequesne
General Motors Co.
Warren, Michigan 48090

ABSTRACT

Generalized root-loci techniques, developed in the mid-70's for squirrel cage motors, have been extended to wound rotor, slip energy recovery systems (static Scherbius drive). In this paper, the influence of a feedback control loop on these root-loci is considered. General conclusions on Scherbius drive dynamics as well as some experimental verifications are also included.

INTRODUCTION

The static Scherbius drive, with its adjustable speed characteristics, is still very much favored for very large drives, because of the lower rating of its electronic components.

While many researchers studied its steady-state capabilities [1], [2], [7] as well as ways to improve them [11], relatively little work was done to assess its dynamics. Since induction motors experience instability in some instances [3], it can be expected that they do also in the Scherbius drive configuration.

Giannakopoulos and Galanos [12], Tsuchiya [13] and Franz and Meyer [15] made digital simulations of such drives. Mittle et al [14] linearized the system equation, but neglected the effect of leakage inductances. The purpose of this research is the investigation of the stability of the Scherbius drive. A general but thorough model is aimed for in order to obtain reliable as well as easy-to-use results.

A first paper [19] proved the theoretical possibility of instability in Scherbius drives. The emphasis in that first paper was, on one hand, to develop a general method of analysis which would encompass a wide variety of machines and drives. On another hand, to use this method to generate a basic set of root-loci yielding general results on dynamic behavior of Scherbius drives.

However, the study was then limited to the open-loop case, where the firing-angles of the thyristors of the inverter and thus the rotor voltage were kept constant during perturbations. The purpose of this paper, is, on one hand, to extend the analysis to the closed-loop case, where the firing angles of the thyristors (hence the rotor voltage) are linked to variations of speed, in ways which are explained in more details below. On another hand, it describes some experimental work aimed at verifying the theoretical derivations.

SYSTEM CONFIGURATION

The system that is being studied is presented in Figure 1.

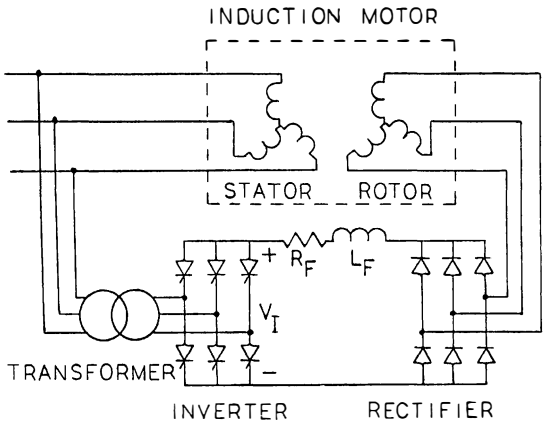

Figure 1: System Configuration

The speed of the drive is directly related to the wound rotor voltage. In turn, the level of that voltage is set and controlled by a rectifier-inverter energy recovery loop and more specifically by the firing-angles of the thyristors of the inverter.

ANALYTICAL APPROACH

The equations of the system are written in a synchronous reference frame, in order for the impedance terms to be time independent [19]. The incremental effects of saturation as well as rotor current harmonics are ignored. Voltages and currents are written with d-q components; this allows a compact formulation with complex numbers; their real and imaginary parts represent the direct and quadrature axes components, respectively.

The steady-state complex equations are written in terms of the complex, operational impedances

0275-9306/86/0000-0510 $1.00 © 1986 IEEE

$\bar{Z}_{so}$, $\bar{Z}_{mo}$, $\bar{Z}_{do}$ and $\bar{Z}_{ro}$. They link voltages (v) and currents (i), on one hand; torques (electrical, T; load, T_L) and rotor speed (ω_r) on another-hand (all notations are defined in the Appendix):

$$\bar{v}_{so} = \bar{Z}_{so}\,\bar{i}_{so} + \bar{Z}_{mo}\,\bar{i}_{ro} \qquad (1)$$

$$\bar{v}_{ro} = \bar{Z}_{do}\,\bar{i}_{so} + \bar{Z}_{ro}\,\bar{i}_{ro} \qquad (2)$$

$$T = n\,M\,\mathrm{Im}\,(\bar{i}_{so}\,\bar{i}_{ro}^{*}) = \frac{J}{N}\,p\omega_r + T_L \qquad (3)$$

Rectifier-inverter loop equation (note about the firing-angle γ: $90° < \gamma < 180°$):

$$|\bar{v}_{so}|\,\cos\gamma = -|\bar{v}_{ro}| + \frac{\pi^2}{18}\,R_F\,|\bar{i}_{ro}| \qquad (4)$$

The open loop dynamic analysis which follows is based on a small perturbations derivation, where terms are allowed to vary slightly around their steady-state values. Using the so-called generalized root-loci theory [6], [8], [9], the number of parameters which the dynamic equations finally depend upon is reduced to a small set of non-dimensional terms. This set of parameters, some of them original to the Scherbius drive [19], [20] is not only small, but its terms vary over small ranges, allowing a systematic study of dynamic behavior.

CLOSED-LOOP DYNAMICS

Block Diagram

The dynamics of the drive can be characterized by the transfer function associating speed variations to load torque variations ($\Delta\omega_r/\Delta T_L$). The open-loop block-diagram is represented on Figure 2. T and T_L are the electric and load torques, respectively; J is the inertia, n is the number of poles pairs:

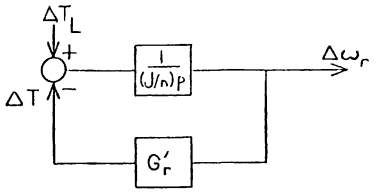

Figure 2: Open-Loop Block-Diagram

The characteristic equation is then:

$$1 + \frac{1}{\frac{J}{n}\,p}\,G'_r = 0 \qquad (5)$$

In the closed-loop, an additional link exists between electric torque and speed, which leaves G'_r unchanged and leads to the following representation:

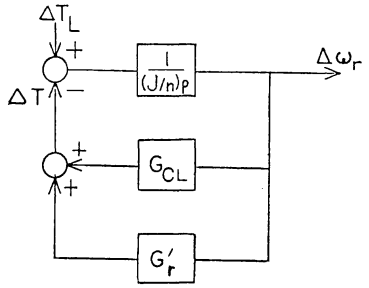

Figure 3: Closed-Loop Block-Diagram

The result is a new characteristic equation:

$$1 + \frac{1}{\frac{J}{n}\,p}\,G'_r\,G_{CL} = 0 \qquad (6)$$

The proof of these statements follows: It consists chiefly in the calculation of the transfer function $\Delta T/\Delta\omega_r$ and of G_{CL}.

Closed-Loop Torque-Speed Relation

The open-loop torque-speed characteristics of Scherbius drives are as follows [1], [2], [19]:

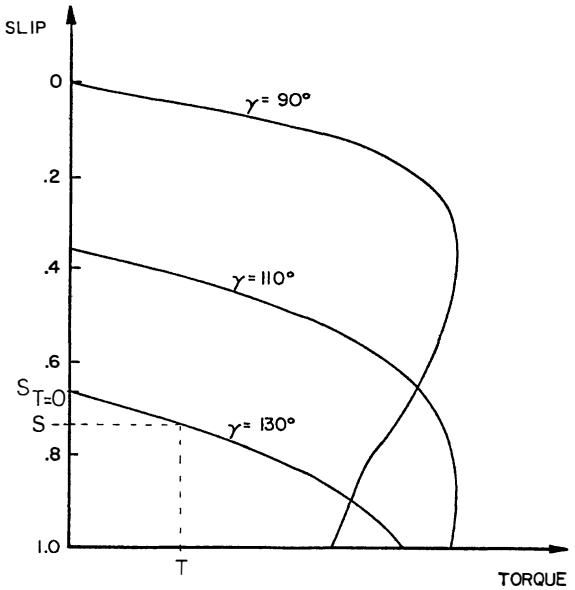

Figure 4. Torque-Speed Characteristic

Each curve corresponds to various loads for a given firing-angle of the thyristors. At no-load, the slip (then denoted $S_{T=O}$) can be approximated by [19].

$$S_{T=O} = -\frac{L_s}{M}\cos\gamma \qquad (7)$$

where L_s and M are respectively the d-q self and mutual inductances of the stator of the machine.

Normal operation takes place at lower torques (relative to peak torque). Then the characteristics are to some extent parallel. Therefore, the open-loop torque depends primarily on the difference between actual and no-load slips (denoted respectively S and $S_{T=O}$) and depends little on the firing-angles. This difference can be called S_{rel} (relative slip);

$$S_{rel} = S - S_{T=O} \qquad (8)$$

If the speed is perturbed then:

$$\Delta S_{rel} = \Delta S - \Delta S_{T=O} \qquad (9)$$

where the prefix Δ denotes a small variation of the corresponding term. Since $S_{T=O}$ depends on the firing-angle (eq. 7), then:

$$\Delta S_{T=O} = \frac{L_s}{M}\sin\gamma\ \Delta\gamma \qquad (10)$$

Because S_{rel} is linked to the torque (see Fig. 4), eq. 9 links variations of torque (through ΔS_{rel}), speed (through the slip variation ΔS) and firing-angle (through $\Delta S_{T=O}$). A closed-loop can hence modify the basic torque-speed characteristic provided a relation of the following sort is created:

$$\Delta\gamma = k_\gamma\ \Delta\omega_r \qquad (11)$$

where ω_r is the rotor speed and k_γ some constant.

Dynamic Equations

If the small perturbation theory is applied to the steady-state equations described earlier, one obtains a set of dynamic equations, to which eq. 11 should be added. They will allow the calculation of the transfer function $\Delta T/\Delta\omega_r$ (see Figure 3):

$$\Delta\bar{v}_s = 0 = \bar{Z}_s\ \Delta\bar{i}_s + \bar{Z}_m\ \Delta\bar{i}_r \qquad (12)$$

$$\Delta\bar{v}_r = \bar{Z}_d\ \Delta\bar{i}_s + \bar{Z}_r\ \Delta\bar{i}_r + M i_{soq}\ \Delta\omega_r \qquad (13)$$

$$\Delta T = nM\ \mathrm{Im}\ (\bar{i}_{ro}\ \Delta\bar{i}_s - \bar{i}_{so}^{*}\ \Delta\bar{i}_r) \qquad (14)$$

$$-|\bar{v}_{so}|\ \sin\gamma\ \Delta\gamma = \Delta|v_r| + \frac{\pi^2}{18} R_F\ \Delta|i_r| \qquad (15)$$

$$\Delta\gamma = k_\gamma\ \Delta\omega_r \qquad (11)$$

All notations are described in the Appendix. In particular, i_{soq} is the q-axis component of stator current if the d and q axes are defined as is explained now.

The rectifier is a passive load to the wound rotor. Therefore, the rotor power ($\bar{v}_{ro}\bar{I}_{ro}^{*}$) is real and the two phasors $\bar{v}_{ro}$ and $\bar{I}_{ro}$ are colinear. The d-q axes system can be chosen to be such that they lie on the d axis; then, they both are real terms. At the same time, it simplifies the equations to assume that the d-q axes move, during the dynamics, in unison with the stator voltage phasor $\bar{v}_s$. First, it allows to write that $\Delta\bar{v}_s = 0$, since the magnitude of $|\bar{v}_s|$, that is the line voltage, is also constant. Secondly, it allows to bring in an equation linking the phase variations of rotor voltage and current in a more simple way.

Because their respective phasors remain colinear, the rotor current ($\Delta\theta_i$) and voltage ($\Delta\theta_v$) phase shifts are equal in magnitude:

$$\Delta\theta_v = \Delta\theta_i = \Delta\theta \qquad (16)$$

Eq. 16 along with the choice of position for the d axis (along v_{ro} and i_{ro}) allows to read simple expressions for the variations of rotor current and voltage, namely:

$$\Delta i_r = \Delta(|\bar{i}_r|\ e^{j\theta}) = \Delta|\bar{i}_r| + j i_{ro}\ \Delta\theta \qquad (17)$$

Sign considerations, based on the fact that energy leaves the rotor imposes $\bar{v}_r$ to be of opposite direction to $\bar{I}_r$ (hence the phase π in the steady-state):

$$\Delta\bar{v}_r = \Delta(|\bar{v}_r|e^{j\pi}) = -\Delta|v_r| + j\ |v_{ro}|\ \Delta\theta \qquad (18)$$

This expression of $\Delta\bar{v}_r$ enables to split eq. 13 into its real part, where it is combined with eqs. 15 and 11, resulting in eq. 19, on one hand; into its imaginary part, (eq. 20), on another hand. Altogether the system becomes:

$$\Delta\bar{v}_s = 0 = \bar{Z}_s\ \Delta\bar{i}_s + \bar{Z}_m\ \Delta\bar{i}_r \qquad (12)$$

$$-\Delta|\bar{v}_r| = |\bar{v}_{so}|\sin\gamma\ k_\gamma\ \Delta\omega_r + \frac{\pi}{18} R_F\ \Delta|\bar{i}_{ro}| = \mathrm{Re}(\bar{Z}_d\ \Delta\bar{i}_s + \bar{Z}_r\ \Delta\bar{i}_r) + M i_{soq}\ \Delta\omega_r \qquad (19)$$

$$|v_{ro}|\ \Delta\theta = \mathrm{Im}(\bar{Z}_d\ \Delta\bar{i}_s + \bar{Z}_r\ \Delta\bar{i}_r) \qquad (20)$$

$$\Delta T = nM \text{ Im } (\bar{i}_{ro} \Delta\bar{i}_s - \bar{i}_{so}^* \Delta\bar{i}_r) \quad (21)$$

The speed variation appears only in eq. 19; in the open-loop (that is when $k_\gamma = 0$), there is only one such term ($Mi_{soq} \Delta\omega_r$). In the closed-loop, this term becomes:

$$(Mi_{soq} - k_\gamma |\bar{v}_{so}| \sin\gamma) \Delta\omega_r$$

and this is actually the only form which is altered by the presence of a closed-loop.

The calculations are aimed at expressing $\Delta T/\Delta\omega_r$. Since the factor multiplying $\Delta\omega_r$ is the only term changed from open-loop to closed-loop, one can conclude that the closed-loop transfer function $\Delta T/\Delta\omega_r$ differs from its open-loop counterpart only by a factor (expressed below so as to be equal to 1 when $k_\gamma = 0$:

$$G_{CL} = 1 - k_\gamma \frac{|v_{so}| \sin\gamma}{Mi_{soq}} \quad (22)$$

This justifies the block-diagram shown on Figure 3.

Characteristic Equation

The closed-loop characteristic equation is then:

$$1 + \frac{1}{\frac{J}{n} p} G_{CL} G'_r = 0 \quad (23)$$

with G_{CL} a constant (eq. 22) and G'_r a rational fraction in p (derivative operator) which is unchanged from the open-loop case. A practical consequence of these developments is that a root-locus drawn in the open-loop case, with a characteristic equation gain varying from 0 to infinity, will also describe the closed-loop case. The exact location of the modes will depend on the existence and the nature of the feed-back loop. Therefore, the general loci presented in [19] apply to the closed-loop case as well.

Conclusion on Dynamics

From the analysis of general root-loci already published [19] and some further investigations of the same nature [20], one can point out several factors affecting the dynamics of Scherbius drives:

Instability is more frequent for small values of (ωT_r) where ω is the supply frequency and T_r the overall rotor time constant (which includes the resistance of the windings as well as that of the filter and connections):

$$T_r = (R_r + \frac{\pi^2}{18} R_F)/\sigma L_r \quad (24)$$

A larger $|\cos\gamma|$ improves stability for a given drive. It can be noticed that it corresponds to a larger rotor voltage and hence a larger electric power load for the machine's rotor.

The time constant of the modes is roughly proportional to:

$$1 + \frac{2}{18} \frac{L_F}{\sigma L_r} \quad (25)$$

This corresponds to the fact that a larger filter inductance (L_F) slows down the transients. This disadvantage must be headed off with larger harmonic current losses.

The time constant is also proportional to the rotor time constant T_r described above.

The closed-loop gain (k_γ) modifies the position of a drive on its root-locus.

EXPERIMENTAL WORK

A Scherbius drive was built with the following characteristics:

Induction machine:
5 hp; 1725 rpm; Stator 220 V, 16A; Rotor 126V, 18.8 A; d,q axes $R_s = 0.25\Omega$; $L_s = 35.4$ mH;
M = 20 mH; $R_r = 0.27\Omega$; $L_r = 12.5$ mH.
Load: 7.5 hp dynamometer, J = 0.03 kgm^2
Rectifier: 6 diodes bridges
Filter: 2 inductances, 75 mH, 0.52Ω each
Inverter: 2 half-wave, three thyristors bridges for power utilization as well as regeneration.
Control: open-loop (V_I = constant)

Four cases were studies corresponding to two values of inverter voltage V_I (see Figure 1) and two values of filter inductances L_F.

Table I: Four cases studied

	Case 1	Case 2	Case 3	Case 4
V_I(V)	75	50	75	50
L_F(mH)	37.5	37.5	75	75

The load torque was perturbed by reducing, for a very short time, the resistance loading the dynamometer, giving an approximate Dirac function. The speed response was then read on a scope as shown on Figure 5 for case 1:

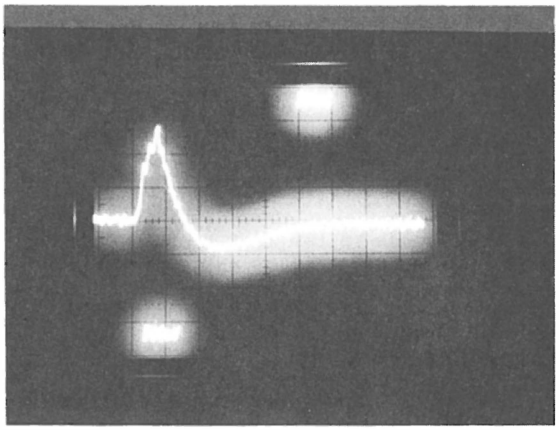

Figure 5: Speed Response (case 1)

The oscillations can be characterized by their frequency and by their envelope, which follows a curve of the type $\mu e^{-t/r}$ (μ, magnitude; r, time constant). This data can be calculated theoretically from the modes of the system obtained from the linearized dynamic equations. A comparison yields the following table where the first number is the calculated one and the second one, in parentheses, is its experimental counterpart.

Table II: Experimental and Theoretical Results

	Case 1	Case 2	Case 3	Case 4
Frequency (Hz)	3.4 (2.8)	3.7 (2.5)	2.3 (2.0)	2.4 (2.3)
Time Constant (μs)	89 (320)	91 (313)	138 (375)	143 (341)
Magnitude (rpm)	35.3 (32)	44.2 (29.1)	41.7 (36.3)	47.2 (36.5)

Frequency and magnitude were predicted with relatively good accuracy. The time constant predictions were slightly optimistic, possibly because of two factors:

1) The ommission of saturation and rotor harmonics
2) The difficulty in assessing the overall rotor resistance with the desired precision.

Two interesting points were noted during the experiments. First, small loads lead to discontinuous DC currents, which in turn lead to higher speeds than otherwise expected. The answer to this problem may be to design carefully the rectifier-inverter and its filter, but this may lead to a prohibitive filter inductance and also incidently to the second problem: any element added in the rotor adds to the effective rotor resistance and may alter the speed-torque characteristic, yielding a poor speed regulation (relatively to usual induction motor drives and speed regulations).

CONCLUSION

The generalized root-loci theory as applied to the static Scherbius drive yields good results, when compared to experiments. Thanks to a small set of nondimensional parameters, it is possible to assess rapidly and with reliability the dynamics of such a drive.

A feedback loop linking variations of firing-angles to variations of speed simply changes the position of the modes on the root-locus concerning the given drive.

APPENDIX 1: DEFINITIONS AND SYMBOLS

The machine impedances are defined in a d-q axis frame under their operational form as follows:

$$\bar{Z}_s = R_s = L_s p + jL_s\omega \quad (26)$$

$$\bar{Z}_m = Mp + jM\omega \quad (27)$$

$$\bar{Z}_r = R_r + L_r p = jL_r\omega_s \quad (28)$$

$$\bar{Z}_d = Mp + jM\omega_s \quad (29)$$

The terms in p vanish when steady-state values (denoted by subscript o) are considered.

Notations

i	a.c. currents
i_{soq}	stator, steady-state, q axis component of current
J	inertia
k_γ	closed-loop gain
L	self-inductance
M	mutual inductances
n	number of pairs of poles
p	derivative operator
R	resistances
s	slip
T	electric torque
T_L	mechanical torque
v	a.c. voltages
V_I	direct inverter voltage (see Fig.1)
$\bar{Z}$	complex impedances (see above)
γ	firing-angle of thyristors
θ	phase shifts
σ	$\sigma = 1 - M^2/(L_r L_s)$
ω	stator current radian frequency

ω_r electric rotor velocity

ω_s rotor current radian frequency

Subscripts

d direct axis

q quadrature asix

r rotor

s stator

o steady-state

F filter parameters (see Fig. 1)

$|\bar{z}|$, $Re(\bar{z})$, $Im(\bar{z})$, and $\bar{z}^*$ denote respectively, the modulus, the real part, imaginary part, and conjugate of the complex entity $\bar{z}$.

REFERENCES

[1] A. Lavi and R.J. Polge, "Induction Motor Speed Control with Static Inverter in the Rotor," IEEE Transactions on Power Apparatus and Systems, vol. PAS-85, no. 1, 1966.

[2] W. Shepherd and J. Stanway, "Slip Power Recovery in an Induction Motor by the Use of a Thyristor Inverter," IEEE Transactions on Industry and General Applications, vol. IGA-5, no. 1, pp. 74-82, 1969.

[3] R. H. Nelson, T. A. Lipo, P. C. Krause, "Stability Analysis of a Symmetrical Induction Machine," IEEE Transactions on Power Apparatus and Systems, vol. PAS-88, no. 11, pp. 1710-1717, 1969.

[4] T. Hori and Y. Hiro, "The Characteristics of an Induction Motor Controlled by a Scherbius System (Application to Pump Drive)," IEEE Industry Applications Society Annual Meeting Conference Record , pp. 775-782, 1972.

[5] H. W. Weiss, "Adjustable Speed AC Drive Systems for Pump and Compressor Applications," IEEE Transactions on Industry Applications, vol. IA-10, no. 1, 1974.

[6] D. W. Novotny, J. H. Wouterse, "Induction Machine Transfer Functions and Dynamic Response by Means of Complex Time Variables," IEEE Transactions on Power Apparatus and Systems, vol. PAS-95, no. 4, pp. 1325-1335, 1976.

[7] G. A. Smith, "Static Scherbius System of Induction-Motor Speed Control," Proceedings IEE, vol. 124, no. 6, pp. 557-560, 1977.

[8] R. Stern and D. W. Novotny, "A Simplified Approadh to the Determination of Induction Machine Dynamic Response," IEEE Transactions on Power Apparatus and Systems, vol. PAS-97, no. 4, pp. 1430-1439, 1978.

[9] A. R. Miles and D. W. Novotny, "Transfer Functions of the Slip-Controlled Induction Machine," IEEE Transaction on Industry Applications, vol. IA-15, no. 1, pp. 54-62, 1979.

[10] A. R. Miles and D. W. Novotny and J. Betro, "The Effect of Volts/Hertz Control on Induction Machine Dynamics," IEEE Industry Applications Society Annual Meeting Conference Record, 1979.

[11] V. Pavlov, H. Okitsu, T. Suzuli, and T. Ohnishi, "Hybrid Speed-Control System of Wound-Rotor Induction Motor," Proceedings IEE, vol. 126, no. 9, pp. 821-825, 1979.

[12] G. Giannakopoulos and G. Galanos, "Dynamic Simulation of an Induction Motor Drive with DC Link in the Rotor Circuits," IEEE Power Engineering Society Winter Meeting, Paper A79112-4, 1979.

[13] T. Tsuchiya, "Suboptimal Control of a Static Scherbius Induction Motor System Using a Microprocessor," IEEE Transactions on Industry Applications. vol. IA-16, no. 5, pp. 686-699, 1980.

[14] V. N. Mittle, K. Venkatesan, and S. C. Gupta, "Stability Analysis of a Constant Torque Static Slip-Power-Recovery Drive," IEEE Transactions on Industry Applications, vol. IA-16, no. 1, pp. 119-126, 1980.

[15] P. Franz and A. Meyer, "Digital Simulation of a Complete Subsynchronous Converter Cascade with 6/12-Pulse Feedback System," IEEE Transactions on Power Apparatus and Systems, vol. PAS-100, no. 12, pp. 4948-4957, 1981.

[16] C. P. Lemone and T. Takeishi, "Large Ajjustable Speed Drives," IEEE Power Engineering Society Summer Meeting, Paper 81SM416-7, 1981.

[17] M. Abbas, and D. W. Novotny, "The Stator Voltage-Controlled Current Source Inverter Induction Motor Drive," IEEE Transaction On Industry Applications, vol. IA-18, no. 3, pp. 219-230, 1982.

[18] K. Fukazawa and D. W. Novotny, "The Influence of Volts/Hertz Control on Filter Impedance Effects in VSI-fed Induction Machines," IEEE Transactions on Industry Applications, vol. IA-18, no. 3, 1982.

[19] B. Lequesne and A. R. Miles, "Generalized Root-Loci Theory for the Static Scherbius Drive," IEEE Transactions on Power Apparatus & Systems, vol. PAS-103, no. 6, 1984.

[20] B. Lequesne "Some Aspects of the Operation of Double-Fed Induction Machines," Ph.D. dissertation, University of Mo-Rolla, 1984.